© Universiti Tun Hussein Onn Malaysia Publisher's Office

JAMEA

http://penerbit.uthm.edu.my/ojs/index.php/jamea

e-ISSN : 2716-6201

Journal of Advanced Mechanical Engineering Applications

Steel Sleeve Repair Welding on Carbon Steel: Intermetallic Compound (IMC) Formation Based on MIG Welding Quality

Mohamad Faris Mohd Ali[1], M.F Mahmod[1,2*]

[1]Faculty of Mechanical and Manufacturing Engineering,
University Tun Hussein Onn Malaysia, Batu Pahat, 86400, MALAYSIA

[2]Structural Integrity and Monitoring Research Group (SIMReG), Faculty of Mechanical and Manufacturing Engineering, University Tun Hussein Onn Malaysia, Batu Pahat, 86400, MALAYSIA

*Corresponding Author

DOI: https://doi.org/10.30880/jamea.2022.03.02.003
Received 19 July 2022; Accepted 04 October 2022; Available online 13 December 2022

Abstract: Steel sleeve repair usage has increased throughout the world, especially in the oil and gas field. Therefore, the efforts to find the perfect parameter to preserve the steel sleeve repair welding parameter. The aim is to determine the improved MIG welding parameter that enhances the weld quality at the steel sleeve joint by using Scanning Electron Microscopy (SEM) and Energy Dispersive X-ray (EDS) to validate the data of the project. The Vickers microhardness test was done to determine the strength of the weldment zone, IMC layer and steel base zone. The steel sample must go through a cutting, grinding, polishing, and etching process. The most preferred finding is the sample B welding parameter which shows the improved microstructure and medium-range strength compared to the other parameter. Finally, the heat input is the most significant component to determine the welding quality because of the microstructure reaction with the welding current.

Keywords: Steel sleeve repair, MIG welding, carbon steel, welding quality

1. Introduction

Natural gas delivery companies have used pipelines as the transportation method. Despite this, the Oil and Gas company has the most significant impact on the global economy. The pipeline installation and lifespan appear not well maintained. There are over 60% of pipeline failures caused by external damage, which is mechanical. The defects usually occur in cracks, corrosion, environmental cracking, and dentures. Most of the typical methods of repairing a gas leak are to replace the faulty piece of the pipe. However, the gas pump needs to turn off, and the affected section of the line must be vented. However, when no loops are diverting the gas flow, this means cutting off the gas supply to another place, resulting in losses for the user and the transporting company [1]. Due to this matter, the alternative that could help reduce the industry losses and restore the pipeline is steel sleeve repair. These reinforcements are routinely performed in areas where the local thickness loss or gas leakage has been discovered, and venting valves are utilized to keep the gas out of the welding process. Steel sleeve repair commonly uses Metal Inert Gas (MIG) as the welding method [2]. The main issue during the steel sleeve repair is the possibility that the welding arc will excessively penetrate the pipe thickness and cause a perforation, resulting in burn-through and product leakage. A welding procedure has been determined to ensure that the repairs are carried out safely, which involves selecting the best technique and operational parameters.

Weld cracking is a typical pipeline problem. Cracks are the most harmful weld faults. Minor pipeline faults might produce severe fractures after welding. Internal stresses that exceed the weld metal, base metal, or both produce cracking.

*Corresponding author: mfaisal@uthm.edu.my

Cracking faults may act as stress concentration sites, causing fatigue failure and promoting hydrogen-assisted and stress corrosion cracking if left uncontrolled. Such faults enhance the risk of catastrophic in-service failures in welded metal items, such as deep-sea pipelines [3]. Welders may avoid fractures by understanding why they form. In Malaysia, pipeline repair costs may vary due to a lack of skilled workers, which might increase demand. Steel sleeve repair is the lowest since it has been used for centuries and has plenty of skilled personnel [4]. Concerns have been expressed over the availability of primary resources for long-term uses as the industry's natural gas, and oil consumption has expanded. To protect the long-term sustainability of oil and gas, experts have started investigating methods to prevent pipeline failure or leakage during the transmission of raw materials to customers. An alternate solution is shown by pinpointing the potential flaw in the offshore pipeline, which includes all joints. Most sleeve joints are steel. Analyzing the correct steel compositions for sleeve joints based on ASME standards is crucial for diagnosing pipeline faults. Non-destructive testing has been extensively used in the oil and gas sector to investigate the welded microstructure of steel sleeve joints made of carbon steel and stainless steel.

Intermetallic compound (IMC) formation happens between two or more materials that form compounds with specific compositions and crystalline structures. The intermetallic compound generation in metal inert gas welding involves the welding quality between the base metal and the filler. However, when utilizing the MIG welding technique, the weak tensile strength of the connection and the production of brittle intermetallic compounds during the welding process frequently led to failure. Therefore, more study is necessary to better understand intermetallic compound (IMC) generation depending on several factors. In addition, it is essential to determine the optimal setting for the highest quality MIG welds, which corresponds with the creation of intermetallic compound (IMC), and then validate it using Scanning Electron Microscopy (SEM) and Energy Dispersive X-ray (EDS) analysis.

2. The Tested Materials and Research Method

The material utilized in this study was low-carbon steel. The materials' chemical compositions and mechanical properties are shown in Tables 1 and 2, respectively.

Table 1 - Chemical compositions of ASTM A-106 grade B [5]

Material	C	Mn	P	S	Si	Cr	Cu	Mo	Ni	V
Composition (%weight)	0.30 max	0.29-1.06 max	0.035 max	0.035 max	0.10 min	0.40 max	0.40 max	0.15 max	0.40 max	0.08 max

Table 2 - Mechanical properties [6]

Properties	Metric	Unit
Tensile strength	415	Mpa
Yield strength	240	Mpa

The welding was conducted by the MIG method with the ER4047 Al-Si Filler metal and the welding position for steel pipe with a dimension of 2.5 inches for external diameter and 2.0 inches for internal diameter. For sample preparation, the steel pipe is cut into several lengths using a grinding wheel cutting machine. After the cutting process, the pipe sleeve is cut vertically into half. Before starting the welding process, the sample is cleaned with acetone to remove contaminants. After finishing the welding process, the sample was cut into two at the welding part for IMC preparation. All the samples are evenly cut with the size of 2cm each and processed for IMC characterization. The samples need to be hot mounted for scanning electron microscopy (SEM) and energy dispersive x-ray spectrometer (EDS). Next, the samples undergo a grinding and polishing process until the surface shows a clear surface for microstructure observation. In order to finish the microstructure observation, the samples are next through the etching process. The etching process is necessary to reveal the metal’s microstructure through the Nital chemical solution. Lastly, the samples are ready for scanning electron microscopy for microstructure observation reaction between the experiment's parameters. Through scanning electron microscopy (SEM), the samples were observed with different magnifications for microstructure formation between different parameters.

Fig. 1 illustrates the schematic of the welding zone observed microstructure which are the welding zone, IMC layer, and base metal area. Fig. 3 shows the sample A microstructure of the weldment, IMC layer, and steel base. The result of the microstructure observation in this study has been etched with 2% nital for 7.5 seconds. The hardness spotted points of the sample in the weldment zone, intermetallic compound layer, and base metal from points 1 to 5 are illustrated in Fig. 2

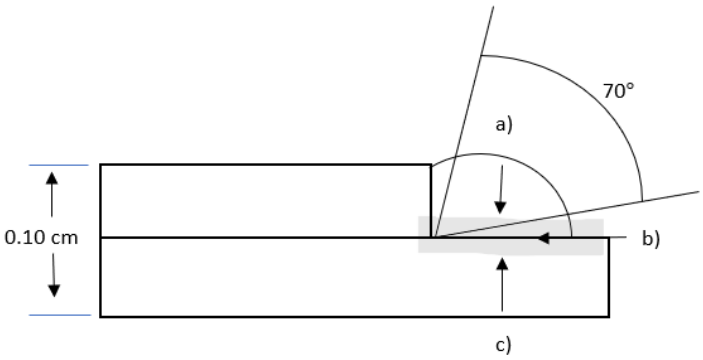

Fig. 1 - Schematic of the welding zone of observed microstructure

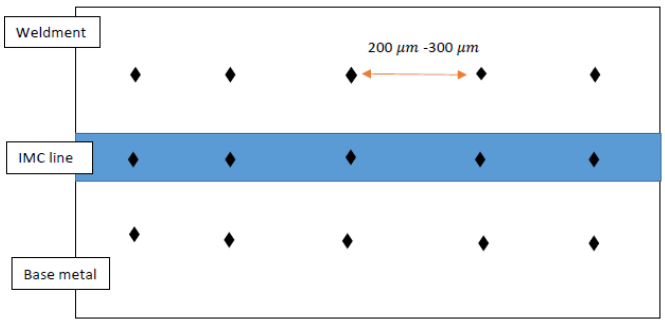

Fig. 2 - Microhardness plot point position on the sample

Table 3 summarizes the chemical compositions of ER4047 Al-Si Filler metal by weight percentage. The sample is tested using three MIG welding parameters: welding current, voltage, and travel speed, whereas silicon shows the highest composition at 12%. In this research, three samples are used with three different weld parameters: welding current, voltage, and travel speed, as in Table 4.

Table 3 - Chemical compositions of ER4047 Al-Si Filler metal [7]

Material	Al	Si	Fe	Cu	Mn	Mg	Zn
Composition (%weight)	Bal.	12	0.8	0.30	0.15	0.10	0.20

Table 4 - Parameter of the experiment

Sample	Welding current (Amp)	Voltage (Volt)	Travel speed (mm/min)
A	100	18	60
B	110	22	90
C	120	24	120

3. Result and Discussion

3.1 Changes in Microstructure

Observation of microstructure using an optical microscope and scanning electron microscope was conducted to find out the changes in the microstructure of the sample that occurs due to heating during the welding process (MIG). Fig. 3(a)-(c) shows the microstructure image of sample A with three section areas with the weldment area zone, the IMC layer, and the based metal area. The grain size of the microstructure is finer. Fig. 3(d) shows the 50x IMC layer microstructure of the intermetallic compound layer which is martensite as the rapid cooling of the austenite form of iron at such a high rate that carbon atoms do not have time to diffuse out of the crystal structure in large enough quantities to form cementite [7].

Fig. 4(a)-(c) shows the microstructure image of sample B with three section areas with the weldment area zone, the IMC layer, and the based metal area. As can be seen from figure 3(b), the microstructure is partially coarse because of the intersection between the weldment and the base metal area. Figure 3(b) shows the 50x IMC layer microstructure of

the intermetallic compound layer, which is ferrite and pearlite, which indicates the slow cooling rate in an iron-carbon system at the eutectoid point in the Fe-C phase [8]. As seen in figure 4(d), the grain size of the microstructure is coarse.

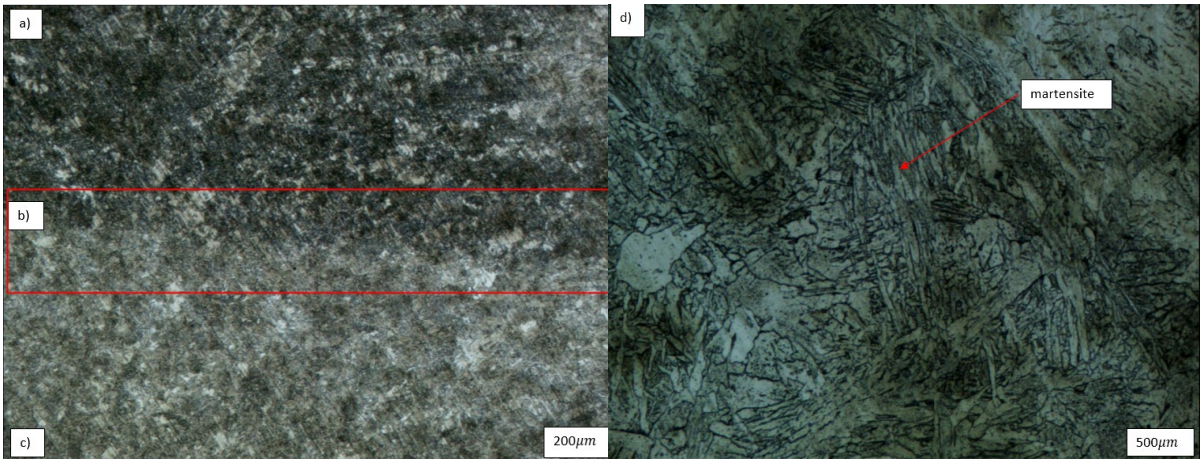

Fig. 3 - Sample A microstructure of (a) weldment zone; (b) IMC layer; (c) base metal at 20x and; (d) 50x magnification

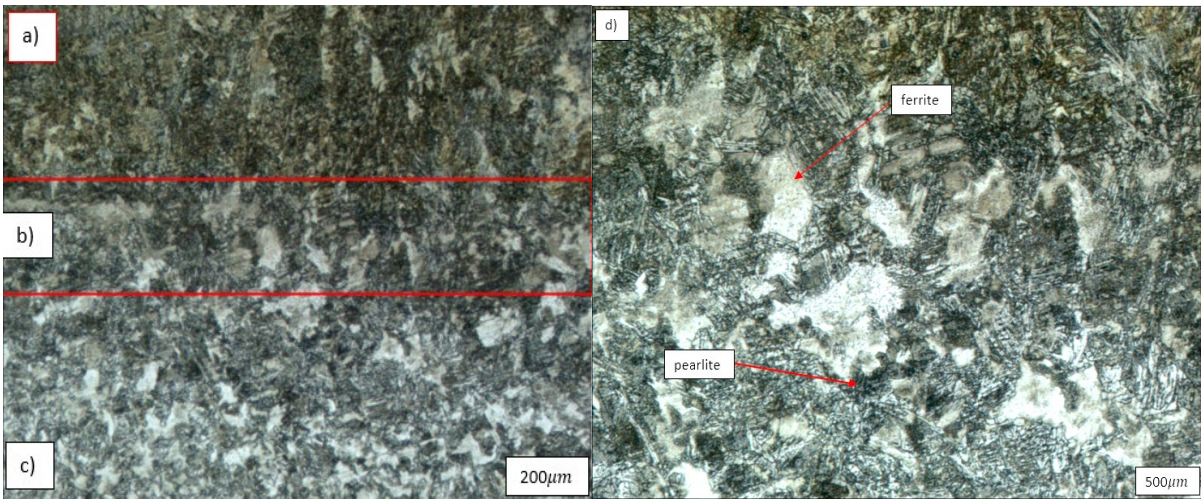

Fig. 4 - Sample B microstructure of (a) weldment zone; (b) IMC layer; (c) base metal at 20x and; (d) 50x magnification

Fig. 5 indicates the microstructure of the IMC layer, whereas the microstructure is 80% coarser because of the intersection between the weldment and the base metal area. Fig. 5(d) shows the 50x IMC layer microstructure of the intermetallic compound layer, which is ferrite and pearlite, due to the high heat input during the MIG welding process. It proves that when the heat input increases, the microstructure size of the weld area becomes coarser as the size of grains becomes bigger since the greater the amount of heat, the faster the grain growth [9].

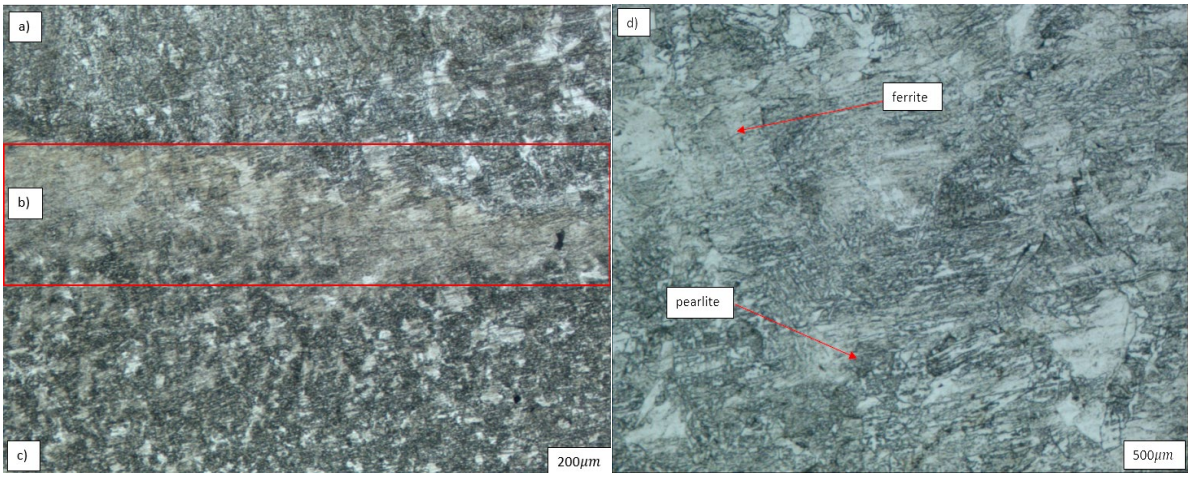

Fig. 5 - Sample C microstructure of (a) weldment zone; (b) IMC layer; (c) base metal at 20x and; (d) 50x magnification

3.2 Chemical Compositions

Data were obtained from the energy dispersive x-ray test of the chemical composition at the weldment, intermetallic compound layer, and base metal. The experimental results reveal that the chemical composition of the sample changes after the metal-inert gas welding process. All the changes in chemical composition may increase the chances of material properties such as cracking. From Table 5, the chemical composition of sample A shows that the carbon and iron content is 6.30% and 93.70%. The chemical composition of sample B shows that the carbon, iron, manganese, and silicon content is 4.47%, 93.55%, 1.33%, and 0.65%. The chemical composition of sample C shows that the carbon, iron, and oxygen content is 9.20%, 83.93%, and 6.86%. The difference between all weld zone chemical compositions occurs because of the interaction between the parent material that has been affected by the welding process, which is not fully melted, which changes the chemical composition of the samples. Therefore, the big data difference between all samples happens due to different parameters used.

Table 5 - Weld zone chemical composition

Material (%weight)	C	Fe	Mn	Si	O
Sample A	6.30	93.70	-	-	-
Sample B	4.47	93.55	1.33	0.65	-
Sample C	9.20	83.93	-	-	6.86

From Table 6, the chemical composition of sample A shows that the carbon, iron, oxygen, silicon, manganese, and calcium content is 8.37%, 68.85%, 17.41%, 2.50%, 2.18%, and 0.69%. The chemical composition of sample B shows that the carbon, iron, oxygen, silicon, manganese and aluminium content is 6.31%, 56.08%, 24.32%, 5.99%, 6.36%, and 0.94%/ The chemical composition of sample C shows that the carbon, iron, oxygen, and silicon content is 9.50%, 66.97%, 18.22% and 4.00%. Intermetallic compound layer chemical composition is different between the samples due to the fusion zone of the welding melted during the welding process in which mixing the parent material and filler. However, due to the different parameters used, which are welding current, voltage, and travel speed, the chemical composition between the samples has different kinds of materials. From Table 7, the chemical composition of sample A shows that the carbon and iron content is 5.74% and 94.26%. The chemical composition of sample B shows that the carbon and iron content is 4.17% and 95.83%. The chemical composition of sample C shows that the carbon and iron content is 4.41% and 95.59%.

Table 6 - Intermetallic compound layer chemical composition

Material (%weight)	C	Fe	O	Si	Mn	Ca	Al
Sample A	8.37	68.85	17.41	2.50	2.18	0.69	-
Sample B	6.31	56.08	24.32	5.99	6.36	-	0.94
Sample C	9.50	66.97	18.22	4.00	-	-	-

Table 7 - Base metal chemical composition

Material (%weight)	C	Fe
Sample A	5.74	94.26
Sample B	4.17	95.83
Sample C	4.41	95.59

3.3 The Vickers Microhardness Result

The sample's mechanical properties depend not only on its chemical composition but also on its microstructure. The microstructure depends on the work process, especially in the heat treatment process [10]. Table 8 shows the Vickers microhardness value of the sample. It is observed that the hardest part of the sample is in sample A intermetallic compound layer area. This is because the welding current for sample A is the lowest, making the cooling rates faster, and the microstructure is martensite, which is uniform and fine. This tendency is affected by a higher carbon and iron content in chemical composition. The combination of carbon and iron in sample A with a carbon content of 8.5% and iron content of 68.85%, is the highest value among the other samples, resulting in the highest microhardness value. As a result, the hardness sample increased [11].

Table 8 - Vickers microhardness test

Sample	Average HV for weldment area	Average HV for IMC area	Average HV for base metal area
Sample A	177.76	179.09	178.41
Sample B	173.03	176.56	169.98
Sample C	159.80	160.87	162.40

While the weldment area of sample B and sample C are lower because carbon and iron content are much lower than in sample A. The average value of the hardness for sample A which are weld zone, intermetallic compound layer, and base metal is 177.76 HV, 179.09 HV, and 178.41 HV. The sample B average value of the hardness for the weldment zone, intermetallic compound layer, and base metal is 173.03 HV, 176.56 HV, and 169.98 HV. The sample C average value of the hardness for the weldment zone, intermetallic compound layer, and base metal is 159.80 HV, 160.87 HV, and 162.40 HV. Fig. 6 shows the tabulated data of all samples' intermetallic compound layer hardness. Sample C has the lowest hardness value due to the high welding current. The average microhardness in sample C decreased. The martensite grew more extensive due to the high temperature leading to lower sample hardness.

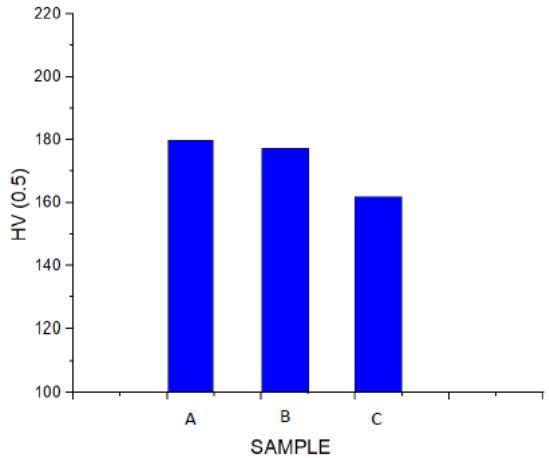

Fig. 6 - Tabulated data of the intermetallic compound layer hardness between all samples

4. Conclusion

From the results and discussion, several findings from this study are concluded as follows:

1. The intermetallic compound was generated between the weldment area and base metal because of the melting and aggregating of the carbon under the action of heating with MIG weld filler. While the current, voltage, and travel speed increased, the microstructure kept growing due to the increase in the welding heat input.

2. The welding current parameter used in this experiment has impacted the welding quality of the sample. The higher welding current will result in low hardness of the material, but the low welding current will result in higher hardness.
3. There are changes in grain size on the weldment area, intermetallic compound layer, and base metal area. In addition, the highest Vickers microhardness value is obtained at sample A, the intermetallic compound, and sample C's lowest. This is because the addition of carbon and iron content in sample A higher compared to both samples B and C. Therefore, the welding quality is affected by the welding parameter chosen due to the microhardness of the material will be determined.

Acknowledgement

The authors would like to thank the Universiti Tun Hussein Onn Malaysia for its financial support through the Tier 1 Research Grant No. H925, and Structural Integrity and Monitoring Research Group (SIMReG) through funding and technical support.

References

[1] H. Phil and A. Cosham,"Pipeline Defect Assessment Manual," *Proceeding of IPC* , vol. IPC02, no. 27067, 2002.

[2] P. S. ION, "Pipeline Pitting and Repair Techniques copy - Pipeline-Pitting-and-Repair-Techniques-copy," vol. 1, 2018.

[3] T. Firdaus, A. M. Asyraf Azmi, and R. Bahar, "Economic Analysis of using E-Glass Composite Wrap Repair System for Pipelines in Malaysia," *Australian Journal of Basic and Applied Sciences*, vol. 8, no. 15, pp. 241–245, 2014.

[4] C. T. Mgonja, "The Consequences of cracks formed on the Oil and Gas Pipelines Weld Joints," Dar es Salaam Institute of Technology Tanzania, vol. 54, 2017.

[5] Y. Wang Y and P. B. Prangnell P.B, "The significance of intermetallic compounds formed during interdiffusion in aluminum and magnesium dissimilar,"*Materials Characterization*, vol. 134, pp. 84–95, 2017.

[6] L. M. Shah, A. Gerlich and Y. Zhou, "Design guideline for intermetallic compound mitigation in Al-Mg dissimilar welding through addition of interlayer," *Int J ADV Manuf Technol*, vol. 94, no. 2667–2678., 2018

[7] J. Kang, C. Wang, G.D. Wang, "Microstructural characteristics and impact fracture behavior of a high-strength low-alloy steel treated by intercritical heat treatment", *Materials Science and Engineering: A*, vol. 553, pp 96-104, 2012.

[8] S. Lars-Eric, "Control of Microstructures and Properties in Steel Arc Welds," Library of Congress Catalog-ing-in-Published Data, British, 1994.

[9] Y.Yang, M. Wei, "Intermetallic compound catalysts_ synthetic scheme, structure characterization and catalytic application," *J. Mater and A. Chem*, vol. 8, pp. 2207-2221, 2020.

[10] O. Grong and O. M. Akselsen, "HAZ Grain Growth Me-chanism in Welding of Low Carbon Microalloyed Steels," *Acta Metallurgica*, 2000.

[11] Z. Wan, H. P. Wang, N. Chen, M. Wang and B. E. Carlson, "Characterization of intermetallic compound at the interfaces of Al-steel resistance spot," *Journal of Materials Processing technology*, vol. 242, pp. 12-23, 2017.